IEEE Access
Multidisciplinary | Rapid Review | Open Access Journal

Received March 18, 2019, accepted April 26, 2019, date of publication May 3, 2019, date of current version May 21, 2019.

Digital Object Identifier 10.1109/ACCESS.2019.2914707

Novel MIMO Detection With Improved Complexity for Near-ML Detection in MIMO-OFDM Systems

SEUNG-JIN CHOI[1], SEONG-JOON SHIM[1], YOUNG-HWAN YOU[2], JAESANG CHA[3], AND HYOUNG-KYU SONG[1]

[1]Department of Information and Communication Engineering, Sejong University, Seoul 05006, South Korea
[2]Department of Computer Engineering, Sejong University, Seoul 05006, South Korea
[3]Department of Electronics and IT Media Engineering, Seoul National University of Science and Technology, Seoul 01811, South Korea

Corresponding author: Hyoung-Kyu Song (songhk@sejong.ac.kr)

This work was supported by the Institute for Information and Communications Technology Promotion (IITP) Grant funded by the Korean government (MSIT) (Development of Immersive Signage Based on Variable Transparency and Multiple Layers) under Grant 2017-0-00217.

ABSTRACT In this paper, a novel efficient algorithm for MIMO detection in MIMO-OFDM systems has been proposed. This paper also shows that the complexity can be greatly reduced by applying the threshold in the breadth-first tree search algorithm step to eliminating paths. That is, this algorithm derives thresholds based on the LR-aided nonlinear algorithm and performs a simple tree search detection algorithm. This algorithm requires a lower computational complexity than the conventional QRD-*M* detection algorithm and achieves the same bit error performance. After the novel detection algorithm is proposed, this paper applies this algorithm to the MIMO-OFDM system for performance comparison in terms of error performance and complexity. In many cases of MIMO-OFDM receivers, the proposed method will be an excellent option for implementation.

INDEX TERMS MIMO systems, OFDM, signal detection, QRD-*M*, BFTS, multiplexing gain.

I. INTRODUCTION

Recently, the wireless communication technology area has been suffered by the rapidly increase of data traffic due to the requirements of the up-to-date applications and a lot of users or devices. The wireless-fidelity (Wi-Fi) and long term evolution (LTE) wireless communication technologies are evolving to obtain higher data throughput and channel capacity, and with the advent of the 5G new radio (NR) era, their importance is becoming even greater [1]–[3]. In wireless communication systems, the increase of data throughput through additional bandwidth and transmission power is very limited due to the lack of radio spectrum and limitations of interference between transmitters. The multiple input multiple output (MIMO) transmission technology has been adopted by a number of wireless communication systems, such as LTE and Wi-Fi, as a way to solve the increase of data throughput [4]. The MIMO system is an antenna technique that increases data throughput or link reliability by using multiple transmit antennas and multiple receive antennas at a base station and terminal. The benefits of the MIMO system are divided into diversity gain that increases link reliability and multiplexing gain that increases data throughput compared to conventional single input single output (SISO) system. The diversity gain can be achieved by transmitting multiple copies of a single bit stream at the transmitter, where the receiver has multiple versions of the same data over different independent paths. The receiver improves link reliability by mitigating the effect of fading through the combining schemes. The multiplexing gain transmits multiple independent data streams, so it can have a channel capacity proportional to the number of antennas used. Thus, the spatial diversity allows the MIMO system to increase the channel capacity without additional bandwidth and transmission power.

The MIMO transmission technique should simultaneously transmit a message causing multiple interference and restore the messages at the receiver. The fundamental object of the receiver is to accurately restore the transmitted original

The associate editor coordinating the review of this manuscript and approving it for publication was Donatella Darsena.

data from the transmitter [5], [23]. This problem is important in the wireless communication areas that require high throughput. The most commonly known detection method for solving detection problems is the maximum likelihood (ML) detection algorithm [6]. The ML method solves the MIMO detection problems based on an exhaustive search algorithm. However, the ML detector increases computational complexity exponentially as multiple antenna architectures or high-order modulation schemes are utilized. Therefore, due to hardware limitations, there is a restriction to implement ML detector. Because of the implementation constraints, the various detection algorithms for signal detection have been studied.

The suboptimal detection algorithm for detecting multiple signals is divided into a linear detection algorithm and a nonlinear detection algorithm [7], [8]. In general, nonlinear methods are imposed with higher computational complexity but achieve better error performance than the linear methods. Representative examples of the linear detection are zero-forcing (ZF) and minimum mean-square error (MMSE) detection algorithms [9]. Typical nonlinear detections include the ordered successive interference cancellation (OSIC), decision-feedback detector (DFD), QR-decomposition based M (QRD-M), sphere decoding (SD) detection algorithms [10]–[16]. The linear methods are based on linear transformation of the received signals. In general, the linear methods are known to have low computational complexity, but there is significant performance loss compared to the ML detector. The interference cancellation (IC) methods, which are nonlinear detection algorithm, generally provide better error performance than linear detection algorithm. The IC based MIMO detection has various variation in design flexibility including the OSIC and DFD. The common drawback of IC based detection methods is error propagation. The tree-search nonlinear methods are the most common detection algorithm studied in the field of multiple antenna systems. The tree-search based MIMO detection has been most studied because the introduction of powerful SD detection algorithm occurs simultaneously with the development of the MIMO system. In addition, some studies have found that the tree-search algorithm has been quite interesting in terms of trade-off between approaching optimal ML performance and reducing computational complexity. The tree-search algorithm is designed to reduce the computational complexity by exploring a limited number of reference signals compared to the optimal ML detector based on the brute-force search. The tree-search detections are categorized into two categories of breadth-first tree-search (BFTS) [11]–[15] and depth-first tree-search (DFTS) [16], [20]–[23]. On the behalf of the BFTS and DFTS, there are QRD-M and SD respectively. Both have the suboptimal performance and low computational complexity compared to ML. They have differences that QRD-M has the fixed computational complexity at all SNRs but SD has the high computational complexity at the low SNR and has low computational complexity when the SNR increases.

TABLE 1. Table of notation in paper.

Definition	Mean
N_T	transmit antennas
N_R	receive antennas
$\boldsymbol{x}$	transmitted signal vector
$\boldsymbol{y}$	received signal vector
$\boldsymbol{n}$	additive white Gaussian noise vector
$\boldsymbol{H}$	complex-valued Rayleigh flat fading channel matrix
$(\cdot)^T$	transpose operator
$\boldsymbol{Q}$	unitary matrix
$\boldsymbol{R}$	upper triangular matrix
$(\cdot)^H$	Hermitian transpose operator
$\widehat{\boldsymbol{y}}$	altered received signal vector
$E^l_{N_T}$	ED of the l-th reference signal of the N_t layer
L	the number of reference signals
M	survival paths
$\tilde{x}$	candidate reference signal of the upper layer metric
η	the threshold for eliminating unnecessary survival paths
$\bar{\boldsymbol{H}}$	channel matrix using the LLL algorithm
$Q(\cdot)$	quantization operation

Especially, SD algorithm is used in the soft-input soft-output MIMO detector [21]–[23] having iterative detection structure to achieve near-capacity and excellent error performance. However, the SD algorithm has high implementation complexity when the number of antennas increases. The lattice-reduction (LR) technique constitutes another detection algorithm that relies on the algebraic concept of the lattice [17]. The Lenstra-Lenstra-Lovász (LLL) algorithm is known as a representative algorithm of the LR technique [18]. In principle, LR technique can further improve error performance by combining with virtually all other MIMO detection algorithms. For example, the LR technique has been used with linear and nonlinear detection algorithms to achieve significant performance improvements with a little additional computational complexity.

As mentioned above, it is important to implement the MIMO detection method with superior performance at the receiver to have a high channel capacity. The QRD-M detection method based on the BFTS algorithm corresponds to the optimal error performance but still has a high implementation complexity because of the multi-antenna architecture and high-order modulation. The proposed algorithm can significantly reduce the complexity of the conventional QRD-M method by further eliminating the survival paths of the BFTS algorithm. It also compares and describes novel detection algorithm with conventional QRD-M algorithm in terms of complexity and performance. Section 2 introduces the MIMO system model and Section 3 describes the conventional QRD-M detection algorithm. The proposed detection algorithm is described in Section 4. In Section 5, the simulation results are illustrated to compare error performance and computational complexity. Section 6 concludes the paper with the conclusion. Table 1 is notations used in this paper.

II. SYSTEM MODEL

The general spatial MIMO system is considered in this paper. Fig. 1 shows a wireless MIMO-orthogonal frequency

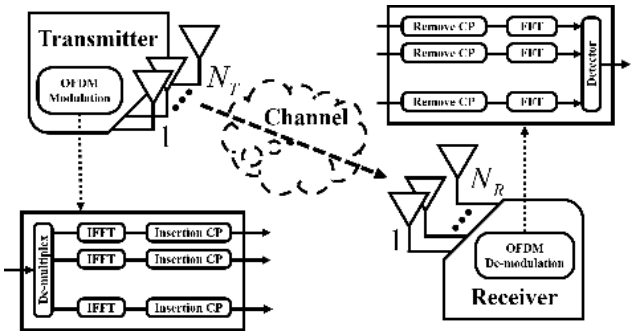

FIGURE 1. The MIMO-OFDM system model.

division multiplexing (MIMO-OFDM) system with N_T transmit antennas and N_R receive antennas to achieve multiplexing gain [19]. The transmission data is demultiplexed into N_T data sub-streams, and each sub-stream is mapped to the phase shift keying (PSK) or quadrature amplitude modulation (QAM) symbol. In this paper, the average power of each symbol is normalized to one for a fair performance comparison. The transmitter generates an OFDM symbol by performing inverse fast Fourier transform (IFFT) and cyclic prefix (CP) insertion for wireless OFDM transmission. The signals transmitted through the N_T antennas are transmitted to the receiver having N_R receive antennas via a wireless channel. In this paper, the subcarrier index is omitted in order to simplify the notation. The received signal at the receiver can be expressed as

$$\boldsymbol{y} = \boldsymbol{H}\boldsymbol{x} + \boldsymbol{n}, \tag{1}$$

where the $\boldsymbol{x} = \begin{bmatrix} x_1 & x_2 & \cdots & x_{N_T} \end{bmatrix}^T \in S^{N_T}$ is $N_T \times 1$ transmitted signal vector. S is the constellation set of each element in $\boldsymbol{x}$. $\boldsymbol{y} = \begin{bmatrix} y_1 & y_2 & \cdots & y_{N_R} \end{bmatrix}^T$ is $N_R \times 1$ received signal vector. The $\boldsymbol{n}$ is the $N_R \times 1$ complex additive white Gaussian noise (AWGN) vector, and the mean and variance are zero and σ_n^2, respectively. And then, $(\cdot)^T$ denotes the transpose operator. Finally, the MIMO channel matrix is as follows

$$\boldsymbol{H} = \begin{bmatrix} h_{11} & h_{12} & \cdots & h_{1N_T} \\ h_{21} & h_{21} & \cdots & h_{2N_T} \\ \vdots & \vdots & \ddots & \vdots \\ h_{N_R1} & h_{N_R2} & \cdots & h_{N_RN_T} \end{bmatrix}, \tag{2}$$

where the element h_{ij} is the channel coefficient between the j-th transmit antenna and the i-th receive antenna and has independent identically distributed (i.i.d.) complex Gaussian distributed coefficients with zero mean and unit variance. The channel matrix $\boldsymbol{H}$ is also a complex-valued Rayleigh flat-fading channel and is perfectly known at the receiver but not at the transmitter.

III. CONVENTIONAL QRD-*M* DETECTION ALGORITHM

This section examines conventional QRD-M detection algorithm for signal estimation in multi-antenna architectures. The first step of this algorithm is to define a new equation through the QR decomposition of the channel matrix $\boldsymbol{H}$ in Eq. (1). The QR decomposition allows to rewrite the system in Eq. (1) as

$$\boldsymbol{y} = \boldsymbol{H}\boldsymbol{x} + \boldsymbol{n} = \boldsymbol{Q}\boldsymbol{R}\boldsymbol{x} + \boldsymbol{n}, \tag{3}$$

where the $\boldsymbol{Q}$ is $N_R \times N_R$ unitary matrix and the $\boldsymbol{R}$ is upper triangular matrix. The received signal $\boldsymbol{y}$ in Eq. (3) is multiplied by $\boldsymbol{Q}^H$ and can be represented as follows,

$$\boldsymbol{Q}^H\boldsymbol{y} = \boldsymbol{Q}^H\boldsymbol{Q}\boldsymbol{R}\boldsymbol{x} + \boldsymbol{Q}^H\boldsymbol{n}, \tag{4}$$

$$\widehat{\boldsymbol{y}} = \boldsymbol{R}\boldsymbol{x} + \widehat{\boldsymbol{n}}, \tag{5}$$

where $\widehat{\boldsymbol{y}} = \boldsymbol{Q}^H\boldsymbol{y}, \widehat{\boldsymbol{n}} = \boldsymbol{Q}^H\boldsymbol{n}$. At this time, the statistical noise characteristic of $\widehat{\boldsymbol{n}}$ is same as $\boldsymbol{n}$. $(\cdot)^H$ denotes the Hermitian transpose operator. The $\widehat{\boldsymbol{y}}$ performs the tree search algorithm on the received signals in the order of breadth first search using the characteristics of the upper triangular matrix $\boldsymbol{R}$.

This algorithm computes the layer metrics between the received signal $\widehat{\boldsymbol{y}}$ and the reference signal candidate $\boldsymbol{c}$, $\boldsymbol{c} = \begin{bmatrix} c_1 & c_2 & \cdots & c_L \end{bmatrix}$, and the layer metrics are computed as

$$E_{N_T}^l = \left| \widehat{y}_{N_T} - R_{N_TN_T} c_l \right|^2, \quad l = 1, 2, \cdots, L, \tag{6}$$

where $E_{N_T}^l$ denotes Euclidean distance (ED) of the l-th reference signal of the N_T-th layer, L is the number of reference signals. Among the L paths, M paths with low ED values are selected as survival paths. The $(L - M)$ unselected paths are removed and are not utilized in the next layer. Therefore, the next layer calculates the accumulated ED between the reference signal candidate and the received signal based on the M survival paths. The formula for the accumulated ED is given by

$$E_{N_T-1}^l = \left| \widehat{y}_{N_T-1} - \left(R_{N_T-1N_T-1} c_l + R_{N_T-1N_T} \tilde{x}_{N_T,P} \right) \right|^2 + E_{N_T,P}, \quad P = 1, 2, \cdots, M, \tag{7}$$

where $E_{N_T,P}$ is the P-th survivor path of the N_T-th layer, $\tilde{x}$ is the candidate reference signal of the upper layer metric. As a result of Eq. (7), a total of $(L \times M)$ accumulated ED values are generated, and M survival paths are selected in the same way as in the N_T-th layer. And then, the $(L \times M) - M$ unselected paths are removed.

The same operation is repeated up to the first layer for signal estimation. The recursive algorithm to be performed up to the first layer is shown as follows,

$$E_i^l = \left| \widehat{y}_i - \left(R_{ii} c_l + \sum_{k=i+1}^{N_T} R_{ik} \tilde{x}_{k,P} \right) \right|^2 + E_{i+1,P}, \quad i = N_T - 1, N_T - 2, \cdots, 1, \tag{8}$$

where i is the layer index. After this algorithm is performed up to the first layer, the QRD-M detector determines the reference signal candidate set of the survival paths having the smallest accumulated ED value as the final estimated signal.

Fig. 2 shows the tree structure of the conventional QRD-M ($M = 2$) method with QPSK in a 4×4 multi-antenna system. The set of black circles $(\tilde{x}_1, \tilde{x}_2, \tilde{x}_3, \tilde{x}_4)$ is the estimated signal

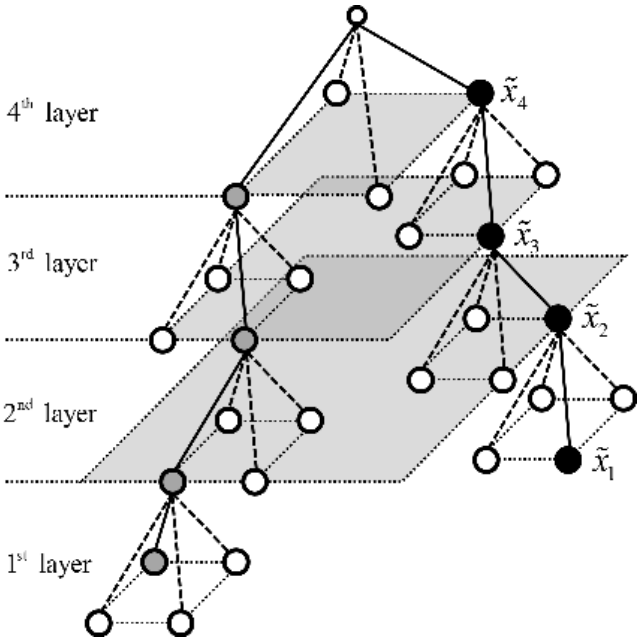

FIGURE 2. The conventional QRD-*M* ($M = 2$) detection algorithm with QPSK in the 4 × 4 system.

obtained the detection, and the gray circle is the candidate set for different reference signals. The solid and dashed lines, respectively, refer to the survival path and the eliminated path.

The QRD-*M* detection algorithm can be used despite an overloaded system. But an overloaded system can cause the performance degradation. The massive MIMO systems that a large number of antennas are used at the transmitter and receiver are one of the important techniques of the 5G wireless communication system. To cancel the other user interference, a block diagonalization method is used. Then, the inter-antenna interference for each user can be canceled by QRD-*M* detection algorithm.

IV. PROPOSED DETECTION ALGORITHM

The proposed detection algorithm reduces the computational complexity while maintaining the similar error performance as the conventional QRD-*M* detection by using the threshold for unnecessary survival paths cancellation. The detection step consists of calculating threshold and eliminating the unnecessary survival paths by threshold. Accurate elimination of unnecessary survival paths can minimize the risk of false detection and gain benefits in terms of complexity.

The proposed method, like the conventional QRD-*M* method, starts from Eq. (5). The BFTS algorithm is performed on the received signal vector $\widehat{\boldsymbol{y}}$. The method obtaining the layer metric is the same as Eq. (6), and the N_T-th layer metric $\tilde{E}_{N_T}$ of proposed method is expressed as follows,

$$\tilde{E}_{N_T}^{l} = \left| \widehat{y}_{N_T} - R_{N_T N_T} c_l \right|^2, \quad l = 1, 2, \cdots, L. \tag{9}$$

In the same way as mentioned above, M survival paths are selected. The threshold η for eliminating unnecessary survival paths is calculated as follows,

$$\eta_{N_T} = \left| \hat{y}_{N_T} - \hat{z}_{N_T} \right|, \tag{10}$$

where η_{N_T} denotes a threshold of the N_T-th layer. The $\hat{y}$ and $\hat{z}$ are generated based on the LR technique. First, the reduced lattice basis $\bar{\boldsymbol{H}} = \boldsymbol{HT}$ is generated by using the LLL lattice reduction algorithm to transform Eq. (3) as follows,

$$\boldsymbol{y} = \bar{\boldsymbol{H}}\boldsymbol{z} + \boldsymbol{n} = \boldsymbol{HT}(\boldsymbol{T}^{-1}\boldsymbol{x}) + \boldsymbol{n}, \tag{11}$$

$$\bar{\boldsymbol{Q}}^H \boldsymbol{y} = \bar{\boldsymbol{Q}}^H \bar{\boldsymbol{Q}} \bar{\boldsymbol{R}} \boldsymbol{z} + \bar{\boldsymbol{Q}}^H \boldsymbol{n}, \tag{12}$$

$$\hat{\boldsymbol{y}} = \bar{\boldsymbol{R}}\boldsymbol{z} + \hat{\boldsymbol{n}}, \tag{13}$$

where $\boldsymbol{T}$ is an unimodular matrix. A detailed description of the complex LLL algorithm is shown in Table 2.

TABLE 2. The complex LLL algorithm.

INPUT: $\boldsymbol{H}$, OUTPUT: $\bar{\boldsymbol{Q}}, \bar{\boldsymbol{R}}, \boldsymbol{T}$

(1) $\left[\bar{\boldsymbol{Q}}, \bar{\boldsymbol{R}}\right] = \mathrm{qr}(\boldsymbol{H})$;

(2) $\delta \in \left(\frac{1}{2}, 1\right)$; $k = 2$; $\boldsymbol{T} = \boldsymbol{I}_{N_T}$;

(3) while $k \le N_T$

(4) for $l = k-1:-1:1$

(5) $\mu = round\left(\bar{\boldsymbol{R}}(l, k) / \bar{\boldsymbol{R}}(l, l)\right)$;

(6) if $\mu \neq 0$

(7) $\bar{\boldsymbol{R}}(1:l, k) = \bar{\boldsymbol{R}}(1:l, k) - \mu \cdot \bar{\boldsymbol{R}}(1:l, l)$;

(8) $\boldsymbol{T}(:, k) = \boldsymbol{T}(:, k) - \mu \cdot \boldsymbol{T}(:, l)$;

(9) end

(10) end

(11) if $\delta \cdot \left|\bar{\boldsymbol{R}}(k-1, k-1)\right|^2 > \left|\bar{\boldsymbol{R}}(k, k)\right|^2 - \left|\bar{\boldsymbol{R}}(k-1, k)\right|^2$

(12) Swap the columns $k-1$ and k in $\bar{\boldsymbol{R}}$ and $\boldsymbol{T}$

(13) $\Theta = \begin{bmatrix} \mathrm{conj}(\alpha) & \beta \\ -\beta & \alpha \end{bmatrix}$ with $\alpha = \frac{\bar{\boldsymbol{R}}(k-1, k-1)}{\left\|\bar{\boldsymbol{R}}(k-1:k, k-1)\right\|}$, $\beta = \frac{\bar{\boldsymbol{R}}(k, k-1)}{\left\|\bar{\boldsymbol{R}}(k-1:k, k-1)\right\|}$

(14) $\bar{\boldsymbol{R}}(k-1:k, k-1:N_T) = \Theta\, \bar{\boldsymbol{R}}(k-1:k, k-1:N_T)$;

(15) $\bar{\boldsymbol{Q}}(k-1:k, k-1:N_T) = \bar{\boldsymbol{Q}}(:, k-1:N_T)\Theta^H$;

(16) $k = \max(k-1, 2)$;

(17) else

(18) $k = k+1$;

(19) end

(20) end

The procedure for obtaining $\hat{z}_{N_T}$ for the η_{N_T} is as follows,

$$\hat{z}_{N_T} = Q\left(\frac{\hat{y}_{N_T}}{\bar{R}_{N_T N_T}}\right), \tag{14}$$

where $Q(\cdot)$ means the quantization operation. Before the next layer is proceeded, the ED value of the survival paths and the threshold is compared. The above procedure means that the survival path where the ED value is larger than the threshold should be removed as an unnecessary path. The path removal using the threshold is not performed in the N_T-th layer, and the BFTS algorithm proceeds to the next layer.

In the $(N_T - 1)$-th layer, the accumulated EDs are calculated based on the M survival paths. The $(N_T - 1)$-th layer metric is expressed as follows,

$$\tilde{E}^l_{N_T-1} = \left|\widehat{y}_{N_T-1} - \left(R_{N_T-1N_T-1}c_l + R_{N_T-1N_T}\tilde{x}_{N_T,P}\right)\right|^2 + \tilde{E}_{N_T,P}, \quad P = 1, 2, \cdots, M. \tag{15}$$

The M survival paths are selected, and the threshold for path elimination is calculated as follows,

$$\eta_{N_T-1} = \left|\hat{y}_{N_T-1} - \hat{z}_{N_T-1}\right| + \eta_{N_T}. \tag{16}$$

Eq. (16) means the accumulated threshold obtained by adding the threshold of the upper layer. The $\hat{z}_{N_T-1}$ is obtained by the following procedure based on the $\hat{z}_{N_T}$ obtained previously.

$$\hat{z}_{N_T-1} = Q\left[\frac{1}{\bar{R}_{N_T-1N_T-1}}\left(\hat{y}_{N_T-1} - \bar{R}_{N_T-1N_T}\hat{z}_{N_T}\right)\right]. \tag{17}$$

The survival paths are compared to the threshold. And then, the survival paths with $\tilde{E}^l_{N_T-1} > \eta_{N_T-1}$ are eliminated. After the removal of the unnecessary paths, the number of new survival paths is defined as M_R, and the value of M is set as $M = M_R$. If the correct survival path is eliminated in the path removal step, the error performance is adversely affected. When too many survival paths are eliminated, the situation that the correct survival path is eliminated may be caused. For this reason, the proposed detection algorithm performs the step of resetting M. When the unnecessary path is eliminated, if the number of remaining survival paths is less than specific value, M is reset to $2M$, and path elimination is performed. The proposed algorithm is repeated from the $(N_T - 1)$-th layer to the first layer based on the Eq. (15) - (17) and the resetting of M. The generalized forms of these three recursive algorithms are as follows,

$$\tilde{E}^l_i = \left|\widehat{y}_i - \left(R_{ii}c_l + \sum_{k=i+1}^{N_T} R_{ik}\tilde{x}_{k,P}\right)\right|^2 + \tilde{E}_{i+1,P}, \tag{18}$$

$$\eta_i = \left|\hat{y}_i - \hat{z}_i\right| + \eta_{i+1}, \tag{19}$$

$$\hat{z}_i = Q\left[\frac{1}{\bar{R}_{ii}}\left(\hat{y}_i - \sum_{j=i+1}^{N_T}\bar{R}_{ij}\hat{z}_j\right)\right], \tag{20}$$

where $i = N_T - 1, N_T - 2, \cdots, 1$.

Finally, in the same scheme as the conventional QRD-M detection, the reference signal candidate set with the smallest accumulated ED is detected as the estimated signal. This detection strategy is superior in terms of computational complexity by reducing the number of survival paths that are calculated when correct path elimination proceeds. Fig. 3 shows a simplified flow chart of the proposed method.

V. SIMULATION RESULTS

This section shows the bit error rate (BER) and computational complexity of the proposed method and compares it with other detection methods. The simulations in this paper are performed on the MIMO-OFDM system and the simulation parameters shown in Table 3 are used.

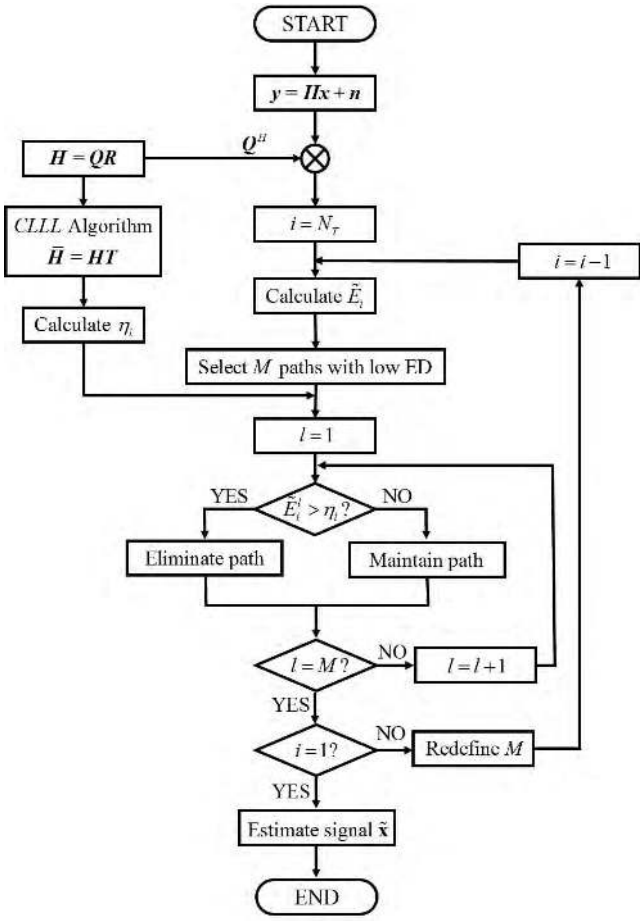

FIGURE 3. The flow chart of the proposed detection algorithm.

TABLE 3. Simulation parameters.

Number of subcarriers	128
CP size	32
Modulation scheme	QPSK, 16-QAM
Channel model	Rayleigh flat-fading channel
Number of path-delay	7
Number of antennas	4 x 4, 8 x 8

To evaluate the proposed method, this paper first describes the simulation results of BER. Fig. 4 and Fig. 5 show the BER simulation results for the 4×4 antenna configuration commonly used in multi-antenna system. Fig. 4 shows the performance of detection algorithms using quadrature phase shift keying (QPSK) modulation. The nonlinear detection, ZF-DFD, is very inferior to other detection algorithms. Also, the effect on the number M of survival paths is clear by comparing the QRD-M detection with different M values to one another. As expected, the QRD-M algorithm illustrates that there is a significant performance penalty as the M value decreases. The LR aided ZF-DFD algorithm has excellent performance while maintaining the difference of about 3.5 dB with the QRD-M ($M = 4$) method unlike the above-mentioned method. SD algorithm also has almost same

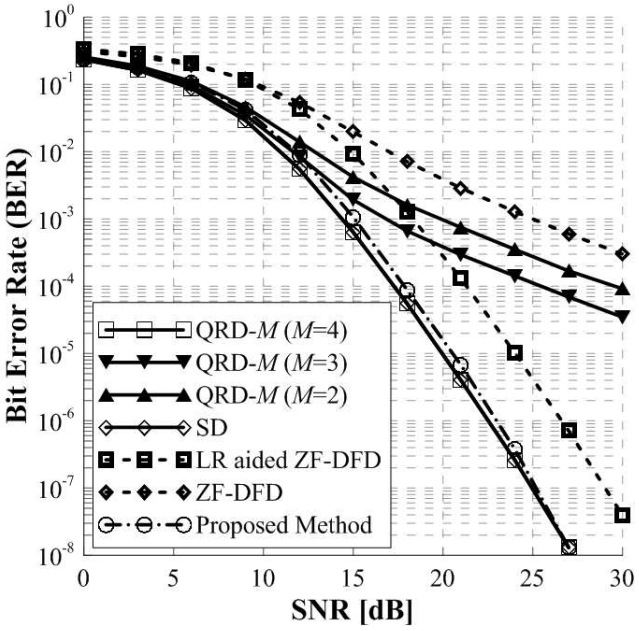

FIGURE 4. BER comparison for 4 × 4 MIMO-OFDM system with QPSK.

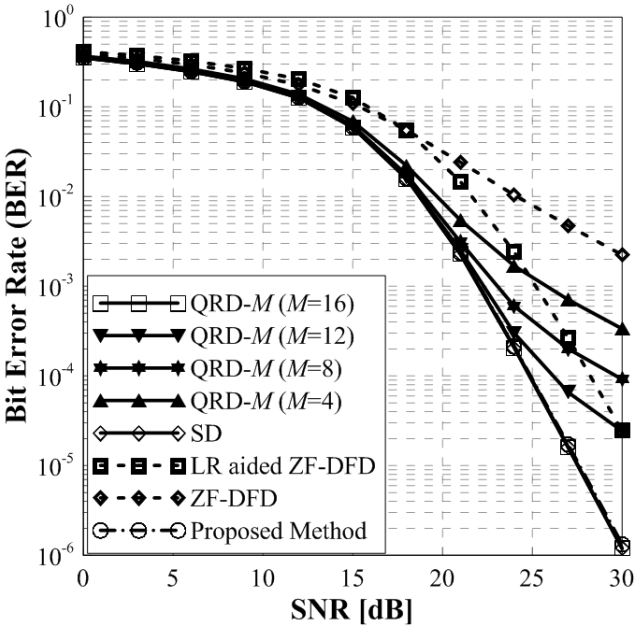

FIGURE 5. BER comparison for 4 × 4 MIMO-OFDM system with 16-QAM.

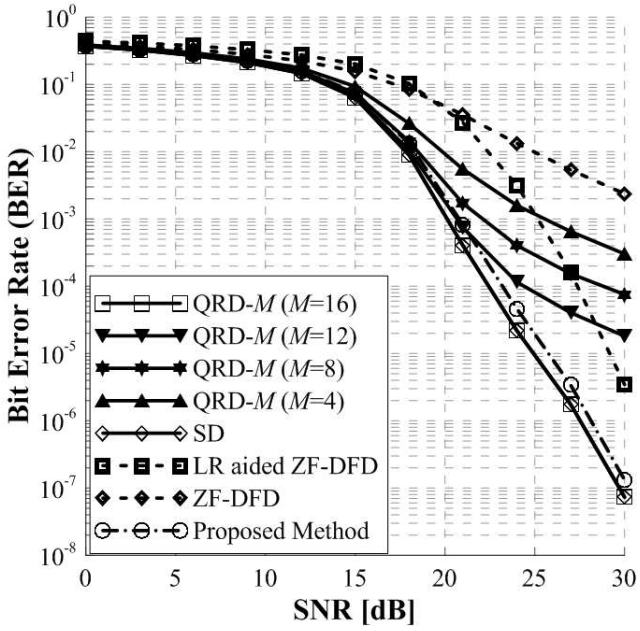

FIGURE 6. BER comparison for 8 × 8 MIMO-OFDM system with 16-QAM.

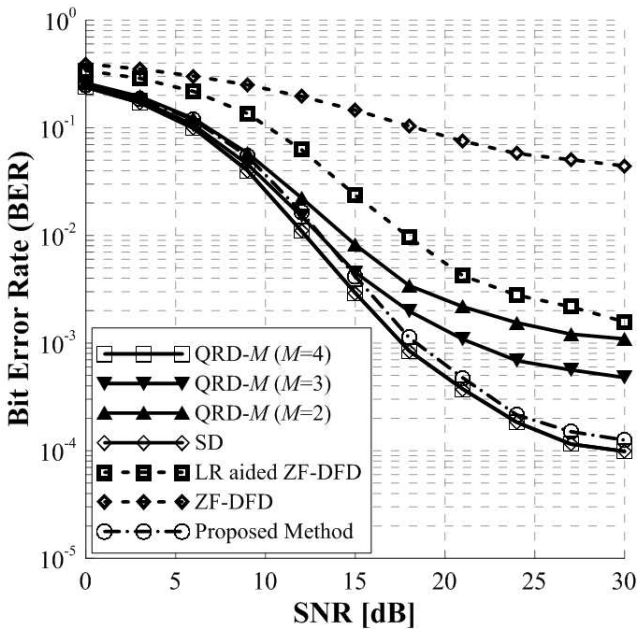

FIGURE 7. BER comparison for 4 × 4 MIMO-OFDM system with QPSK in the non-suppressed ICI.

performance compared to QRD-M ($M = 4$). On the other hand, the proposed detection algorithm has similar performance to the QRD-M ($M = 4$) with suboptimal performance. The proposed method shows a performance difference of approximately 0.5 dB for a BER of 10^{-5}.

Fig. 5 shows the BER performance of the 16-QAM modulation scheme with the same antenna configuration as in Fig. 4. This figure shows the same pattern like the Fig. 4. The QRD-M detection with $M = 16$ shows a suboptimal performance result, and the QRD-M detection with other M values has poor performance. The error performance of the proposed method in Fig. 5 is extremely similar to suboptimal performance. Fig. 6 shows the 8 × 8 antenna system with the 16-QAM modulation scheme. The proposed detection shows a performance degradation of less than 1 dB compared to the QRD-M with $M = 16$. Performance degradation does not occur according to the SNR and suboptimal performance is maintained. The simulation results of the other detection algorithms are similar to that described methods.

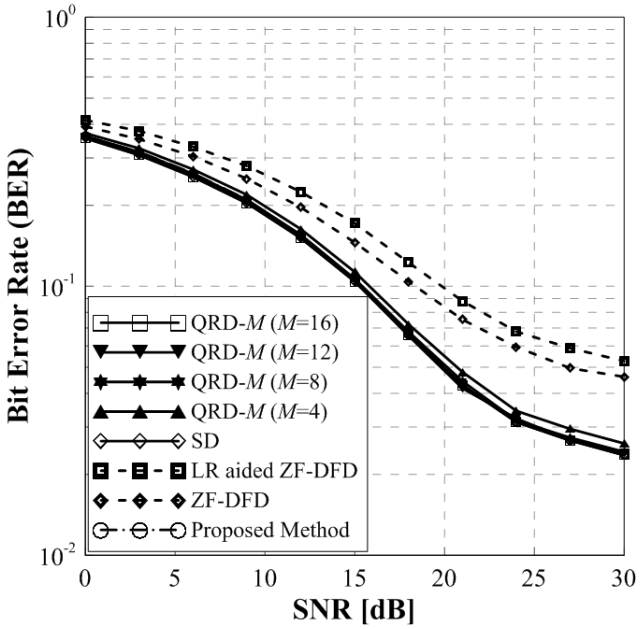

FIGURE 8. BER comparison for 4 × 4 MIMO-OFDM system with 16-QAM in the non-suppressed ICI.

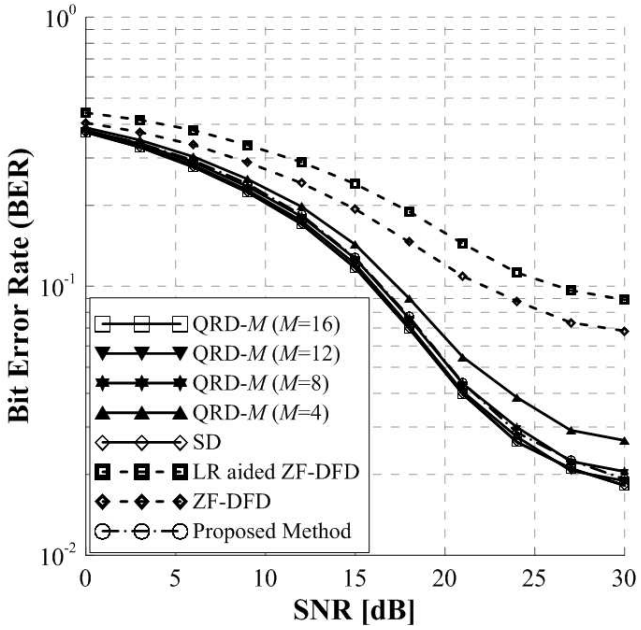

FIGURE 9. BER comparison for 8 × 8 MIMO-OFDM system with 16-QAM in the non-suppressed ICI.

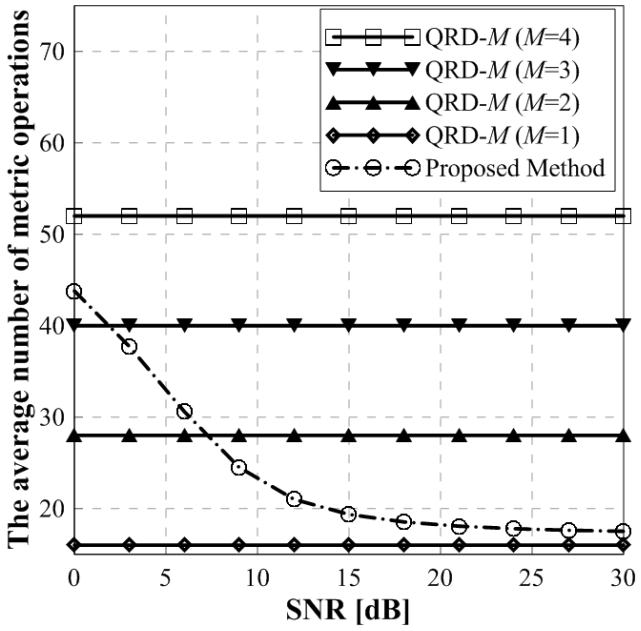

FIGURE 10. The average number of metric operations according to the SNR in 4 × 4 MIMO system with QPSK.

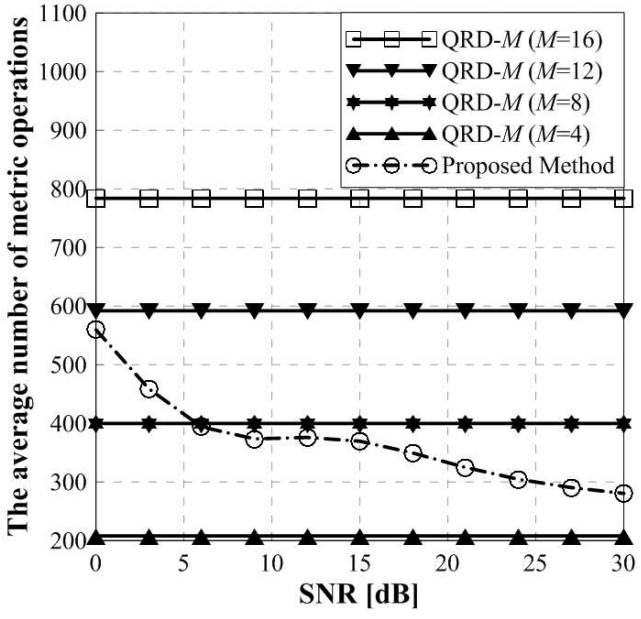

FIGURE 11. The average number of metric operations according to the SNR in 4 × 4 MIMO system with 16-QAM.

Fig. 7-9 are the simulation results for the Fig. 4-6 considering non-suppressed inter-carrier interference (ICI). Simulation results in the presence of non-suppressed ICI have error performance degradation compared to simulation results in Fig. 4-6. However, the proposed detection algorithm has suboptimal error performance despite non-suppressed ICI.

To evaluate the proposed detection algorithm in terms of complexity, Fig. 10-12 show the average number of metric operations. Unlike the conventional QRD-M algorithm with fixed complexity, the proposed algorithm has a metric operation number that varies with SNR due to the elimination of an additional survival paths. Fig. 10, 11, and 12 illustrate the average number of metric operations to compare complexity for the proposed algorithm and the conventional detection algorithms according to the SNR. Fig. 10 compares the complexity of the detection algorithms in 4 × 4 MIMO antenna systems using QPSK modulation. The proposed detection algorithm significantly reduces the number

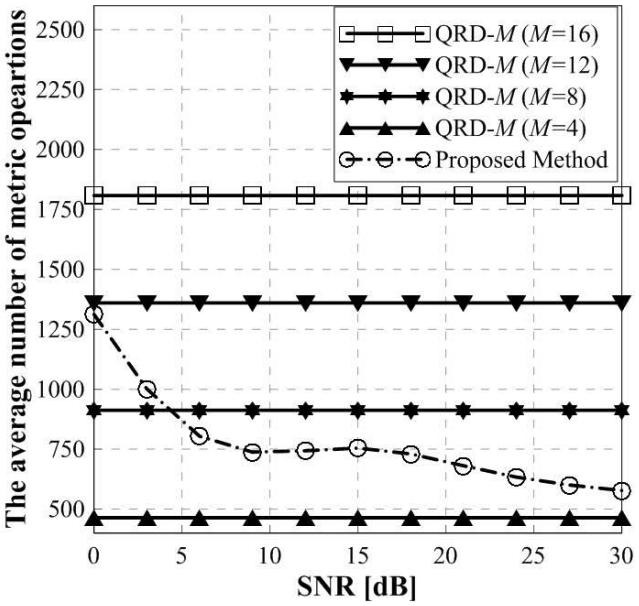

FIGURE 12. The average number of metric operations according to the SNR in 8 × 8 MIMO system with 16-QAM.

of metric operations at the high SNR. The comparison result of the metric operation shows that the proposed algorithm has significantly low complexity over the QRD-M with $M = 4$ in all SNR intervals. When the SNR is about 2 dB and 7.5 dB respectively, the proposed algorithm results in a lower number of metric operations than the QRD-M with $M = 3$ and $M = 2$. When SNR is 30 dB, the number of operations almost reaches the QRD-M ($M = 1$) algorithm and obtains considerable complexity improvement.

Fig. 11 and 12 show the simulation results of 4 × 4 and 8 × 8 MIMO-OFDM systems using 16-QAM modulation, respectively. Both results have a lower number of operations than the QRD-M ($M = 16$) as well as the QRD-M ($M = 12$). From about 6 dB of SNR, the proposed method in Fig. 11 continues to have lower complexity than the QRD-M ($M = 8$). It can be seen that the proposed method in relation to the above-mentioned suboptimal error performance shows superior performance with a very low number of metric operations. The simulation result on the 8 × 8 system also illustrates low complexity like 4 × 4 system.

Table 4 shows the formula of the number of metric operations for the detection algorithms presented in simulation results.

It can be seen that the proposed detection algorithms in the Fig. 10 - 12 have considerable advantages over the conventional QRD-M detection algorithm by significantly reducing the computational complexity. This algorithm has low complexity because it eliminates unnecessary survival paths. It is worth to note, that the path eliminated process is fairly accurate, since there is little error performance degradation caused by reducing the number of metric operations.

Table 5 shows the comparison of average number of metric operations with 16-QAM modulation scheme for the

TABLE 4. The number of metric operations.

Number of Metric Operations of the Detection Algorithms	
SD Detection Algorithm	$\sum_{i=1}^{N} L_i$
QRD-M Detection Algorithm	$2^O + M \times 2^O \times (N_T - 1)$
Proposed Detection Algorithm	$2^O + M_{\text{Mean}} \times 2^O \times (N_T - 1)$

O: Modulation Order
L_i : The number of metric operations at the i-th layer
M_{Mean}: The average number of survival paths from the first layer to the $(N_T - 1)$ layer

TABLE 5. The comparison of average number of metric operations for the suboptimal detection algorithms.

	SNR [dB]	0	6	12
4×4 MIMO System	QRD-M (M = 16)	784	784	784
	SD	2323	977	516
	Proposed Algorithm	559	394	370
8×8 MIMO System	QRD-M (M = 16)	1808	1808	1808
	SD	1309794	180005	36109
	Proposed Algorithm	1312	803	743

TABLE 6. The average number of metric operations and the standard deviation for the proposed detection algorithm.

	SNR [dB]	3	15	27
4×4 MIMO System	μ	468	384	301
	σ	33	49	50
	$(\mu - 3\sigma) \sim (\mu + 3\sigma)$	369 ~ 567	237 ~ 531	151 ~ 451
8×8 MIMO System	μ	1062	838	706
	σ	60	81	84
	$(\mu - 3\sigma) \sim (\mu + 3\sigma)$	882 ~ 1242	595 ~ 1081	454 ~ 958

μ: the average number of metric operations
σ: the standard deviation of metric operations

suboptimal detection algorithms according to SNR and the number of antennas. The QRD-M, SD and proposed detection algorithm have the suboptimal error performance compared to ML detection algorithm. But the QRD-M, SD and proposed detection algorithm have the different number of computational complexity. The QRD-M has the fixed complexity at all of SNR. However, the SD detection algorithm has a low complexity when the SNR increases. The proposed detection algorithm also has a low complexity when the SNR increases. However, the proposed detection algorithm has the low complexity compared to the QRD-M and SD detection algorithms.

Table 6 shows the average number of metric operations and the standard deviation for the proposed detection algorithm according to SNR. Also, the 3σ (σ: the standard deviation of metric operations) interval for the metric operations of proposed detection algorithm is added. As the SNR increases, the average number of metric operations decreases but the standard deviation of metric operations increases.

When the SNR increases, the more paths are eliminated and the complexity is decreased. However, the M value is reset to $2M$ because the correct survival path may be eliminated by repeating the path removal step. Therefore, as the SNR increases, the standard deviation of metric operations increases.

VI. CONCLUSION

This paper proposes the improved QRD-M detection algorithm with low complexity by eliminating unnecessary survival paths. This algorithm uses the LR aided DFE scheme to define the threshold and removes the unnecessary survival paths with the ED larger than the threshold. The proposed method achieves the same error performance as the suboptimal QRD-M method and outperforms in terms of complexity. In this algorithm, the higher the SNR, the more accurate paths can be eliminated. When the SNR is high, the proposed method has a great effect of improving the complexity. It is also possible to provide a trade-off between the computational complexity and error performance by appropriately resetting the M during the path elimination process. Future tasks for this paper can be proceeded in the direction of performing optimal path elimination process. Research on these future tasks can provide better error performance and low complexity. In many cases of the MIMO-OFDM receivers, the proposed method would be the superior option for practical implementation due to the low complexity and good error performance. Also, the proposed method is expected to decrease the computational complexity at the massive MIMO system that a large number of antennas are used.

REFERENCES

[1] D. Astely, E. Dahlman, A. Furuskär, Y. Jading, M. Lisdström, and S. Parkvall, "LTE: The evolution of mobile broadband," *IEEE Commun. Mag.*, vol. 47, no. 4, pp. 44–51, Apr. 2009.

[2] A. Ghosh, R. Ratasuk, B. Mondal, N. Mangalvedhe, and T. Thomas, "LTE-advanced: Next-generation wireless broadband technology," *IEEE Wireless Commun.*, vol. 17, no. 3, pp. 10–22, Jun. 2010.

[3] J. G. Andrews *et al.*, "What will 5G be?" *IEEE J. Sel. Areas Commun.*, vol. 32, no. 6, pp. 1065–1082, Jun. 2014.

[4] G. J. Foschini, "Layered space-time architecture for wireless communication in a fading environment when using multi-element antennas," *Bell Labs Tech. J.*, vol. 1, no. 2, pp. 41–59, Feb. 1996.

[5] P. W. Wolniansky, G. J. Foschini, G. D. Golden, and R. A. Valenzuela, "V-BLAST: An architecture for realizing very high data rates over the rich-scattering wireless channel," in *Proc. URSI Int. Symp. Signals, Syst., Electron.*, Oct. 1998, pp. 295–300.

[6] R. van Nee, A. van Zelst, and G. Awater, "Maximum likelihood decoding in a space division multiplexing system," in *Proc. IEEE 51st Veh. Technol. Conf.*, vol. 1, May 2000, pp. 6–10.

[7] E. G. Larsson, "MIMO detection methods: How they work," *IEEE Signal Process. Mag.*, vol. 26, no. 3, pp. 91–95, May 2009.

[8] S. Yang and L. Hanzo, "Fifty years of MIMO detection: The road to large-scale MIMOs," *IEEE Commun. Surveys Tuts.*, vol. 17, no. 4, pp. 1947–1988, 4th Quart., 2015.

[9] R. Bööhnke, D. Wübben, V. Kühn, and K. D. Kammeyer, "Reduced complexity MMSE detection for BLAST architectures," in *Proc. IEEE Global Telecommun. Conf.*, vol. 4, Dec. 2003, pp. 2258–2262.

[10] G. D. Golden, C. J. Foschini, R. A. Valenzuela, and P. W. Wolniansky, "Detection algorithm and initial laboratory results using V-BLAST space-time communication architecture," *Electron. Lett.*, vol. 35, no. 1, pp. 14–16, Jan. 1999.

[11] M. S. Baek, Y. H. You, and H. K. Song, "Combined QRD-M and DFE detection technique for simple and efficient signal detection in MIMO-OFDM systems," *IEEE Trans. Wireless Commun.*, vol. 8, no. 4, pp. 1632–1638, Apr. 2009.

[12] K. J. Kim, J. Yue, R. A. Iltis, and J. D. Gibson, "A QRD-M/Kalman filter-based detection and channel estimation algorithm for MIMO-OFDM systems," *IEEE Trans. Wireless Commun.*, vol. 4, no. 2, pp. 710–721, Mar. 2005.

[13] J. K. Kim, J. H. Ro, and H. K. Song, "A simplified QRD-M algorithm in MIMO-OFDM system," *IEICE Trans. Fundam. Electron., Commun. Comput. Sci.*, vols. E100, no. 10, pp. 2195–2199, Oct. 2017.

[14] J.-K. Kim, S.-J. Choi, J.-H. Ro, and H.-K. Song, "Adaptive K-best BFTS signal detection algorithm based on the channel condition for MIMO-OFDM signal detector," *IEICE Trans. Fundam. Electron., Commun. Comput. Sci.*, vols. E100, no. 10, pp. 2207–2211, Oct. 2017.

[15] X. Jing, M. Wang, W. Zhou, and H. Liu, "Improve QRD-M detection algorithm for generalized spatial modulation scheme," *Int. J. Antennas Propag.*, vol. 2017, Jan. 2017, Art. no. 3581592.

[16] B. Hassibi and H. Vikalo, "On the expected complexity of integer least-squares problems," in *Proc. IEEE Int. Conf. Acoust., Speech, Signal Process.*, vol. 2, May 2002, pp. 1497–1500.

[17] D. Wübben, D. Seethaler, J. Jaldéén, and G. Matz, "Lattice reduction," *IEEE Signal Process. Mag.*, vol. 28, no. 3, pp. 70–91, May 2011.

[18] A. K. Lenstra, H. W. Lenstra, and L. Lovász, "Factoring polynomials with rational coefficients," *Mathematische Annalen*, vol. 261, no. 4, pp. 515–534, Dec. 1982.

[19] H. Sampath, S. Talwar, J. Tellado, V. Erceg, and A. Paulraj, "A fourth-generation MIMO-OFDM broadband wireless system: Design, performance, and field trial results," *IEEE Commun. Mag.*, vol. 40, no. 9, pp. 143–149, Sep. 2002.

[20] G. Romano, D. Ciuonzo, P. S. Rossi, and F. Palmieri. (Mar. 2013). "Low-complexity dominance-based sphere decoder for MIMO systems." [Online]. Available: https://arxiv.org/abs/1303.0699

[21] G. Papa, D. Ciuonzo, G. Romano, and P. S. Rossi, "A dominance-based soft-input soft-output MIMO detector with near-optimal performance," *IEEE Trans. Commun.*, vol. 62, no. 12, pp. 4320–4335, Dec. 2014.

[22] C. Studer and H. Bölcskei, "Soft-input soft-output single tree-search sphere decoding," *IEEE Trans. Inf. Theory*, vol. 56, no. 10, pp. 4827–4842, Oct. 2010.

[23] P. S. Rossi, G. Romano, D. Ciuonzo, and F. Palmieri, "Gain design and power allocation for overloaded MIMO-OFDM systems with channel state information and iterative multiuser detection," in *Proc. 8th Int. Symp. Wireless Commun. Syst.*, Nov. 2011, pp. 769–773.

SEUNG-JIN CHOI received the B.S. degree in information and communication engineering from Sejong University, Seoul, South Korea, in 2017, where he is currently pursuing the M.S. degree with the Department of Information and Communications Engineering. His research interests include wireless communication system design and MIMO detection.

SEONG-JOON SHIM received the B.S. degree in optical engineering from Sejong University, Seoul, South Korea, in 2018, where he is currently pursuing the M.S. degree with the Department of Information and Communications Engineering. His research interests include wireless communication system design and MIMO signal processing.

YOUNG-HWAN YOU received the B.S., M.S., and Ph.D. degrees in electronic engineering from Yonsei University, Seoul, South Korea, in 1993, 1995, and 1999, respectively. From 1999 to 2002, he was a Senior Researcher with the Wireless PAN Technology Project Office, Korea Electronics Technology Institute (KETI), South Korea. Since 2002, he has been a Professor with the Department of Computer Engineering, Sejong University, Seoul. His research interests include wireless/wired communications system design, spread spectrum transceivers, and system architecture for realizing advanced digital communication systems, especially, for wireless OFDM.

JAESANG CHA received the Ph.D. degree from the Department of Electronic Engineering, Tohoku University, Japan, in 2000. He was with ETRI, from 2000 to 2002, and with Seokyeong University, from 2002 to 2005. Since 2005, he has been a Professor with the Department of Electronics and IT Media Engineering, Seoul National University of Science and Technology, Seoul, South Korea. He also serves as the Head of the IoT Research Center (IoT/IoL ITRC) and the IoT Convergence Research Institute, Seoul National University of Science and Technology. His research interests include wireless communication, the Internet of Signage (IoS), digital broadcasting, the IoT/IoL, OWC, and LED-IT convergence technology.

HYOUNG-KYU SONG received the B.S., M.S., and Ph.D. degrees in electronic engineering from Yonsei University, Seoul, South Korea, in 1990, 1992, and 1996, respectively. From 1996 to 2000, he was a Managerial Engineer with the Korea Electronics Technology Institute (KETI), South Korea. Since 2000, he has been a Professor with the Department of Information and Communications Engineering, Sejong University, Seoul. His research interests include digital and data communications, information theory, and their applications with an emphasis on mobile communications.